JOURNAL OF MATERIALS SCIENCE: MATERIALS IN MEDICINE 7 (1996) 399–402

Bioceramics – simulated body fluid interfaces: pH and its influence of hydroxyapatite formation

P. N. DE AZA, F. GUITIAN, A. MERLOS*, E. LORA-TAMAYO*, S. DE AZA‡
Instituto de Cerámica, Universidad de Santiago de Compostela, Spain
**Centro Nacional de Microelectronica (CSIC), Bellaterra, Barcelona, Spain*
‡Instituto de Cerámica y Vidrio (CSIC), Arganda del Rey, Madrid, Spain

In the present work a method to determine the pH at bioceramics–simulated body fluid interfaces has been developed. The results obtained with several bioactive silica-based bioceramic materials are used to propose a general mechanism for hydroxyapatite formation.

1. Introduction

Apart from hydroxyapatite (HA) implants, one of the conditions for ceramic materials (CM) to be bioactive is to form a HA layer on their surfaces while exposed to simulated body fluid (SBF).

The mechanism of HA formation on bioactive silica-based CM has been studied by different authors [1–3]. All of them claim that a silica hydrogel layer is formed on the surface of the CM prior to the formation of the HA layer. This hydrated silica is responsible for the HA nucleation. However, none of the authors have paid attention to the influence of pH at the CM–SBF interfaces on HA formation, although it is well known that HA is formed at pH values greater than 8 [4, 5].

In the present work a method to determine the pH at bioceramics–SBF interfaces has been developed. The results obtained with several bioactive silica-based CM are used to propose a general mechanism for HA formation.

2. Materials and methods

The following bioactive materials have been used: bioglass ® [6]; $CaO \cdot SiO_2$ glass (CS-glass) [7]; magnesium containing glass (A3) [8] and polycrystalline pseudowollastonite (psCS) [9]. In addition, a non-bioactive $CaO \cdot SiO_2$ glass containing 13 wt % zirconia (W-Z) has also been used [10].

The pH value at the CM–SBF interface was measured using two identical ion-sensitive field effect transistors (ISFET) [11] while the materials were immersed in the SBF [12]. The measurements were made at constant drain to source current and voltage (I_{ds} and V_{ds}). The pair of ISFETs were arranged in a differential measurement set-up (Fig. 1a). The ISFET sensitive membrane consists of a 100 nm thick layer of Si_3N_4 over a 78 nm thick layer of SiO_2. The sensitive area of each chemical sensor is 400×20 μm^2 and the size of the whole chip is $2.4 \times 1.35\,mm^2$ (Fig. 1b).

3. Results and discussion

Fig. 2 shows the variation of pH versus time for all the materials studied. As can be seen all the bioactive materials show a rapid increase in pH at the CM–SBF interfaces which tend to reach pH values greater than 9, and in some cases even 10, after 15 min. However, in the non-bioactive (W-Z) material the pH after 0.5 min remains essentially constant (pH = 7.62).

Fig. 3 shows the variation of pH versus distance from the CM–SBF interface. This indicates that the large increase in pH takes place just at the CM–SBF interface and as soon as we move away from this interface the pH decreases suddenly to the original value of the SBF (7.25).

In all the bioactive materials studied a Ca–P layer similar to that shown in Fig. 4a is formed on their surface above an amorphous silica interlayer (Fig. 4b). In all cases the Ca–P layer has been identified as HA, which is similar to that found in natural bone apatites (Fig. 5)

Fig. 6 shows the range of stability of the different phosphate species versus pH. In the pH interval between 7.21 and 12.3 the predominant species is HPO_4^{2-}. Fig. 7 shows a unified solubility diagram for various Ca phosphates in terms of the predominant ionic species HPO_4^{2-} above pH = 7.21. The calcium

This paper was accepted for publication after the 1995 Conference of the European Society of Biomaterials, Oporto, Portugal, 10–13 September.

0957–4530

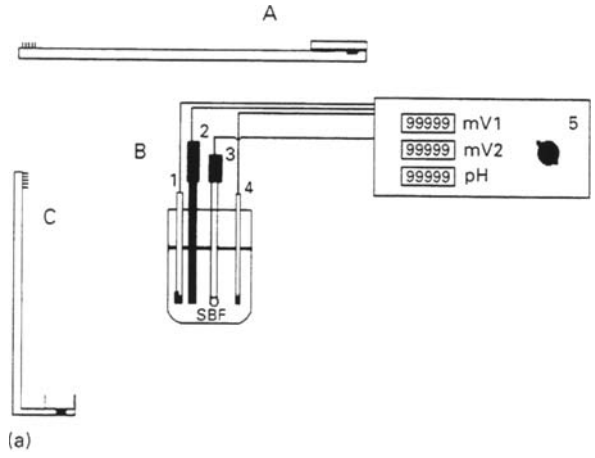

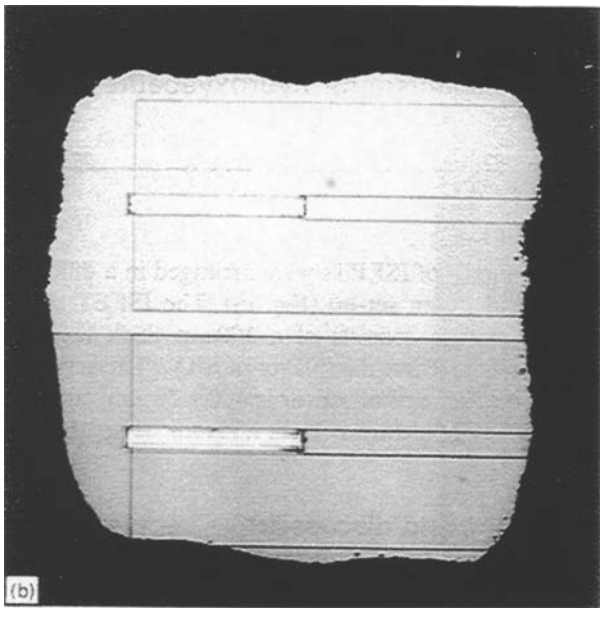

Figure 1 (a) A: ISFET in contact with the sample; B: the pair of ISFETs mounted in a differential measurement set-up, (1) ISFET in contact with the sample, (2) Pt-reference electrode, (3) pH-glass electrode and (4) ISFET in opposition to the other ISFET; C: ISFET in contact with the grounded sample. (b) A view of the ISFET sensitive membrane.

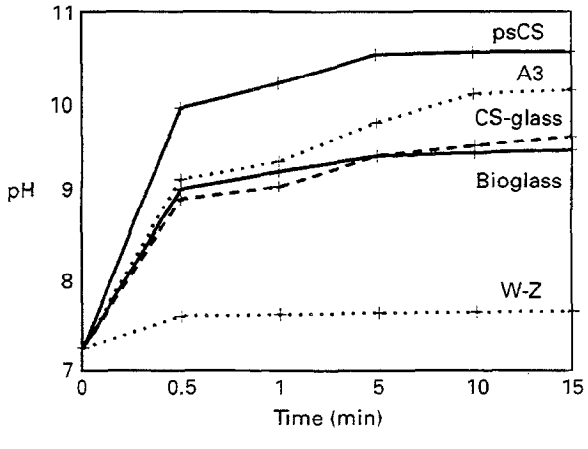

Figure 2 Variation of pH with time for all the material studied.

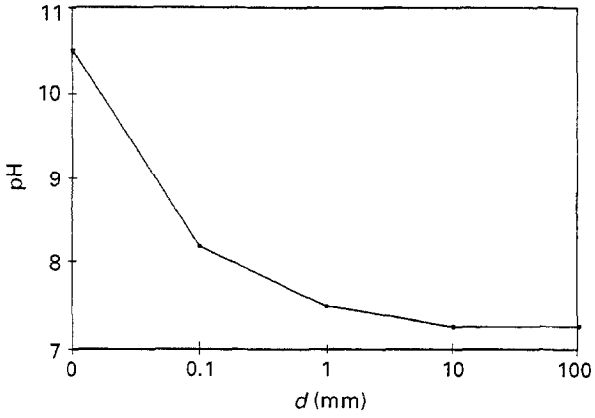

Figure 3 Variation of pH with distance from the material–SBF interface.

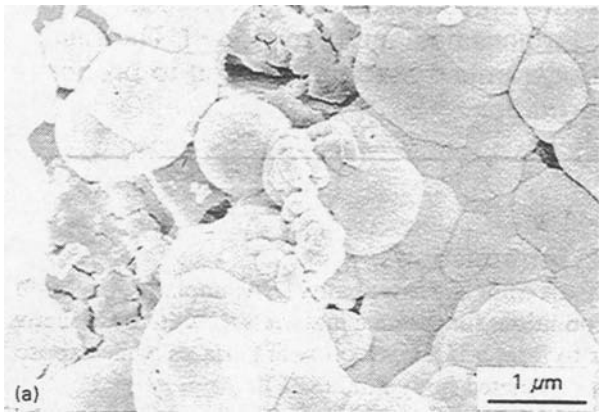

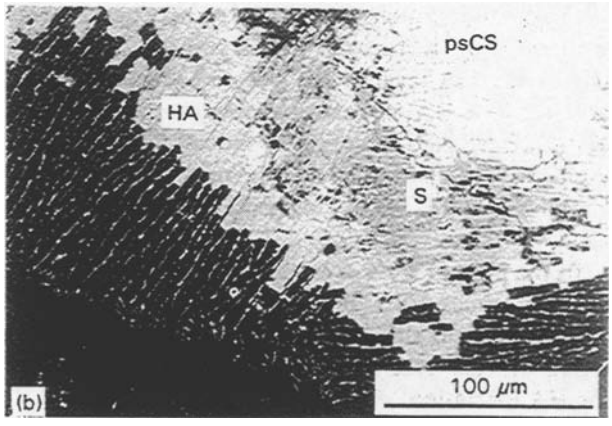

Figure 4 (a) SEM micrograph of the surface of the material psCS after 3 weeks exposure to SBF. (b) SEM microstructure of a cross-section of the material psCS after 3 weeks exposure to SBF: HA hydroxyapatite; S amorphous silica, psCS pseudowollastonite.

phosphates decrease in solubility in the order $CaHPO_4 \cdot 2H_2O$ (brucite) > $CaHPO_4$ (monetite) > $Ca_8H_2(PO_4)5H_2O$ (orthocalcium phosphate) > β-$Ca_3(PO_4)_2$ (β-tricalcium phosphate) > $Ca_5OH(PO_4)_3$ (hydroxyapatite). As can be seen in Fig. 7, at SBF HPO_4^{2-} concentration equal to 10^{-3} M and pH between 9.5 and 10.5 the solution is supersaturated with respect to HA and precipitation takes place. These conditions are reached at the CM–SBF interface.

From Fig. 6 we can see that in the pH range between 9 and 10.5 the predominant species at the

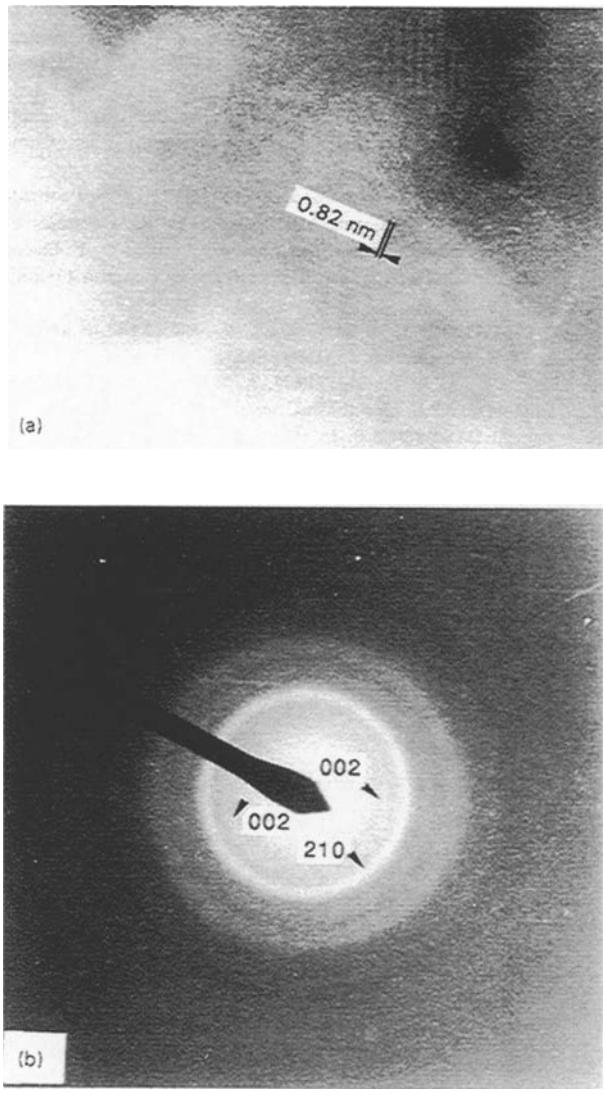

Figure 5 (a) High resolution image of HA crystals shows well resolved (1 0 0) lattice plane image of 0.83 nm spacing. (b) SAD spots showing clear (0 0 2) arc indicating the preferential orientation of the HA.

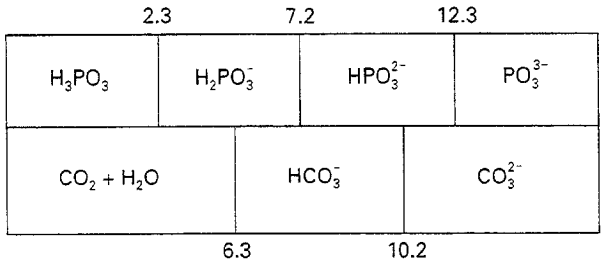

Figure 6 Range of stability of the different phosphate and carbonate species versus pH.

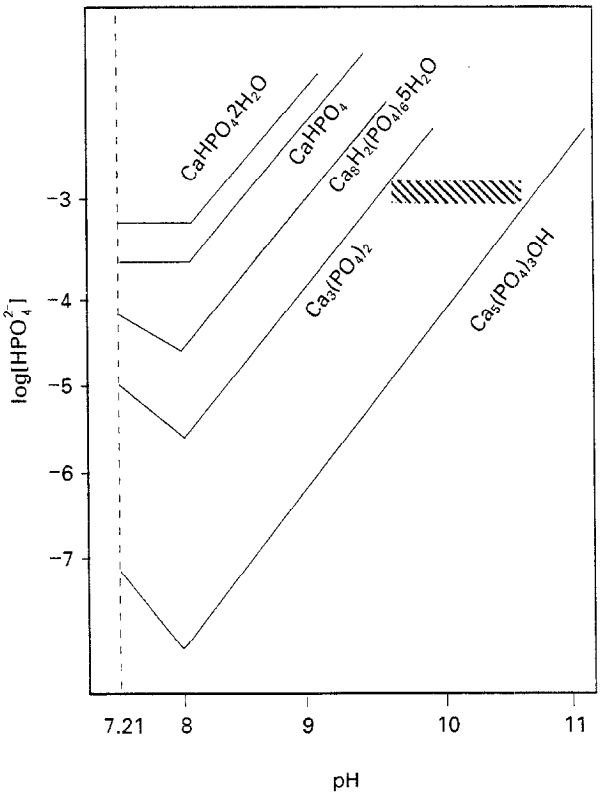

Figure 7 Unified solubility diagram for various Ca phosphate minerals [16].

interface CM–SBF, together with HPO_4^{2-}, can be HCO_3^- or CO_3^{2-}. Consequently both of them can precipitate together with the HA. The presence of CO_3^{2-} in the HA layer has been reported by several authors [13, 14] and confirmed for the present authors by XPS study of the HA layer [15].

Taking into account these results and those previously reported [9] the mechanism of HA formation in bioactive silica-based ceramic materials can be described as follows: At pH 7,25 of the SBF the reaction mechanism starts (in all the materials studied) through an ionic exchange of H_3O^+ from the SBF by labile cations of materials such as Na^+, K^+, Ca^{++}, etc. This induces the formation of an amorphous hydrogel silica layer and a sudden increase in pH from 9 to 10.5 at the CM–SBF interface. This condition determines the partial solution of amorphous silica as SiO_3^{2-} and the subsequent precipitation of HA.

4. Conclusions

When a bioactive silica-based material is immersed in SBF the pH at the CM–SBF interface suddenly increases, reaching values in the range 9 to 10.5. This increase in pH at the interface is mainly due to ionic exchange of H_3O^+ from the SBF for labile cations of materials such as Na^+, K^+, Ca^{++}, etc. This exchange leaves a silica hydrogel layer formed on the CM surfaces prior to the formation of the HA layer. At this high pH value part of the silica hydrogel is dissolved in the SBF and subsequent precipitation of a HA layer takes place on the surface of the materials.

The mechanism found is common for both amorphous and crystalline silica-based bioactive materials studied up until now.

Acknowledgements

This work was supported by CICYT under Project MAT95-0385. In addition, P. N. De Aza thanks the Ministry of Education and Science of Spain for the Fellowship given to her. The authors wish to thank Dr Z. B. Luklinska and Dr M. Anseau for the facilities given to P. N. de Aza during her stay at IRC in Biomedical Materials, The London Hospital, Medical College, University of London. Thanks are also due to Professor L. Hernandez for useful discussions.

References

1. L. L. HENCH, *J. Amer. Ceram. Soc.* **74** (1991) 1487.
2. H. K. KARSSON, K. FRÖBERG and T. RINGBON, *J. Non.-Cryst. Solids* **112** (1989) 69.
3. T. KOKUBO, *ibid.* **120** (1990) 138.
4. Z. BAKÓ and I. KOTSIS, *Ceram. Int.* **18** (1992) 373.
5. C. SANTOS, PhD thesis, Universidad de Santiago, Spain, January 1995.
6. L. L. HENCH, R. J. SPLINTER, T. K. GREENLE and W. C. ALLEN, *J. Biomed. Mater. Res. Symp.* **2** (1971) 117.
7. K. OHURA, T. NAKAMURA, T. YAMAMURO, T. KOKUBO, Y. EBISAWA and M. OKA, *J. Biomed. Mater. Res.* **25** (1993) 1052.
8. J. S. MOYA, A. P. TOMSIA, A. PAZO, C. SANTOS and F. GUITIAN, *J. Mater. Sci. Mater. Med.* **5** (1994) 529.
9. P. N. DE AZA, F. GUITIAN and S. DE AZA, *Scripta Metall. Mater.* **31** (1994) 1001.
10. *Idem. J. Amer. Ceram. Soc.* **76** (1993) 1052.
11. A. MERLOS, I. GARCIA, C. CANE, J. ESTEVE, J. BARTROLI and C. JIMENEZ, in Proceedings of the 5th Conference on Sensors and Their Applications, Edinburgh, September 1991, p. 127.
12. J. GAMBLE, in "Chemical anatomy, physiology and pathology of extracellular fluid" (Harvard University Press, Cambridge, MA, 1967).
13. I. REHMAN, L. L. HENCH and W. BONFIELD, in Proceedings of the 6th International Symposium on Ceramics in Medicine, Philadelphia, November 1993, edited by P. Ducheyne and D. Christiansen (Butterworth-Heinemann Oxford, 1993) p. 123.
14. I. REHMAN, L. L. HENCH, W. BONFIELD and R. SMITH, *Biomaterials* **15** (1994) 865.
15. P. N. DE AZA, F. GUITIAN, A. R. GONZALEZ-ELIPE and S. DE AZA, Unpublished results.
16. W. L. LIMSAY and P. L. ULEK, in "Minerals in soil environments" (Soil Science Society of America, Madison, WI, 1977) p. 639.